http://dx.doi.org/10.5012/bkcs.2014.35.11.3267

Effect of Double Replacement of L-Pro, D-Pro, D-Leu or Nleu in Hydrophobic Face of Amphipathic α-Helical Model Antimicrobial Peptide on Structure, Cell Selectivity and Mechanism of Action

Song Yub Shin

Department of Cellular & Molecular Medicine, School of Medicine, Chosun University, Gwangju 501-759, Korea
E-mail: syshin@chosun.ac.kr
Received July 5, 2014, Accepted July 26, 2014

In order to investigate the effects of the double replacement of L-Pro, D-Pro, D-Leu or Nleu (the peptoid residue for Leu) in the hydrophobic face (positions 9 and 13) of amphipathic α-helical non-cell-selective antimicrobial peptide $L_8K_9W_1$ on the structure, cell selectivity and mechanism of action, we synthesized a series of $L_8K_9W_1$ analogs with double replacement of L-Pro, D-Pro, D-Leu or Nleu in the hydrophobic face of $L_8K_9W_1$. In this study, we have confirmed that the double replacement of L-Pro, D-Pro, or Nleu in the hydrophobic face of $L_8K_9W_1$ let to a great increase in the selectivity toward bacterial cells and a complete destruction of α-helical structure. Interestingly, $L_8K_9W_1$-L-Pro, $L_8K_9W_1$-D-Pro and $L_8K_9W_1$-Nleu preferentially interacted with negatively charged phospholipids, but unlike $L_8K_9W_1$ and $L_8K_9W_1$-D-Leu, they did not disrupt the integrity of lipid bilayers and depolarize the bacterial cytoplasmic membrane. These results suggested that the mode of action of $L_8K_9W_1$-L-Pro, $L_8K_9W_1$-D-Pro and $L_8K_9W_1$-Nleu involves the intracellular target other than the bacterial membrane. In particular, $L_8K_9W_1$-L-Pro, $L_8K_9W_1$-D-Pro and $L_8K_9W_1$-Nleu had powerful antimicrobial activity (MIC range, 1 to 4 μM) against methicillin-resistant *Staphylococcus aureus* (MRSA) and multidrug-resistant *Pseudomonas aeruginosa* (MDRPA). Taken together, our results suggested that $L_8K_9W_1$-L-Pro, $L_8K_9W_1$-D-Pro and $L_8K_9W_1$-Nleu with great cell selectivity may be promising candidates for novel therapeutic agents, complementing conventional antibiotic therapies to combat pathogenic microorganisms.

Key Words : Model antimicrobial peptide, Structure, Cell selectivity, Bacterial-killing mechanism

Introduction

Antimicrobial peptides (AMPs) are non-adaptive host defense components that provide a first line of defense against invading pathogens.[1-3] AMPs are widely distributed in all species ranging from protozoa to vertebrates.[1-3] With the alarming emergence of a number of bacteria that are resistant to conventional antibiotics, antimicrobial peptides are being intensively studied with the objective of developing a novel class of antimicrobial drugs.[1-3] AMPs are classified into cell-selective and non-cell-selective peptides. The cell-selective peptides (*e.g.* magainins and cecropins) selectively kill bacterial cells but not mammalian cells.[4,5] The non-cell-selective (*e.g.* melittin and pardaxin) kill both bacterial and mammalian cells.[6,7] The cell selectivity between AMPs is due to the difference in the interaction between zwitterionic (major component of mammalian cells) and negatively charged (major component of bacterial cells) phospholipids. The non-cell-selective AMPs bind both zwitterionic and negatively charged phospholipid membranes, whereas the cell-selective peptides preferentially bind negatively charged phospholipids. For AMPs to be useful in human and veterinary application, these peptides must have high selectivity toward bacterial cells.

Even though the exact mechanism against target microorganisms of AMPs is not clearly understood, it is generally accepted that it involves interaction of the peptides with the lipid membranes of the target microbe.[8,9] First the positively charged residues of the peptides bound to the negative charged phospholipid of the pathogen mainly the electrostatic interactions. And then, they mostly adapted α-helical structure or β-sheet structure and increased the permeability of the lipid membranes either by ion channel formation or the disruption of lipid bilayers, resulting in the cell death of target cells. In addition, the hydrophobic interactions between hydrophobic residues of the peptide and the lipid acyl chain are essential for their ion channel formation or the disruption of lipid bilayers. Accordingly, amphipathic α-helical LK-model peptides composed of positively charged lysines and hydrophobic leucines have been employed to clarify their modes of action and selectivity between bacterial and mammalian cells.[10-19] Many studies using α-helical LK-model peptides indicated that net positively charge and hydrophobicity of the peptides is sufficient for showing antimicrobial activity and their hydrophobic-hydrophilic balance is a critical factor in controlling the selectivity between bacterial and mammalian cells.[10-19]

In our previous study, in order to develop novel cell-selective peptides having potent antimicrobial activity but no hemolytic activity and investigate their mode of action on bacterial and mammalian cells, we designed and synthesized a perfectly amphipathic α-helical non-cell selective LK-

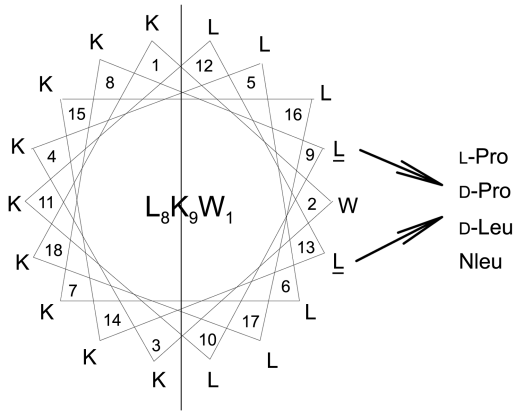

Figure 1. The α-Helical wheel diagrams for non-cell-selective model antimicrobial peptide $L_8K_9W_1$. The line indicates the interface between the hydrophobic face and the positively charged face. Arrows indicate positions 9 and 13 replaced by double L-Pro, D-Pro, D-Leu or Nleu.

model AMP ($L_8K_9W_1$) (KWKKLLKKLLKLLKKLLK-NH_2) composed of hydrophobic residues (Leu and Trp) and positively charged residues (Lys) and its analogs introduced the helix-breaking amino acid such as L-Pro or D-Pro.[20] This study revealed that the incorporation of L-Pro or D-Pro into the hydrophobic face of non-cell-selective $L_8K_9W_1$ resulted in a drastic reduction in hemolytic activity, while retaining their good antimicrobial activity.[20]

In the present study, to investigate the effects of the double replacement of L-Pro, D-Pro, D-Leu or Nleu (the peptoid residue for Leu) in the hydrophobic face of $L_8K_9W_1$ on the structure, cell selectivity (human red blood cells *versus* bacterial cells) and molecular mechanism, we designed and synthesized a series of $L_8K_9W_1$ analogs with double replacement of L-Pro, D-Pro, D-Leu or Nleu in the hydrophobic face (positions 9 and 13) of $L_8K_9W_1$ (Figure 1 and Table 1). The cell selectivity of the peptides was evaluated by assessing their antimicrobial activity against Gram-negative bacteria and Gram-positive bacteria and their hemolytic activity against human red blood cells. Circular dichroism (CD) spectroscopy was employed to determine peptide secondary structures in membrane-mimicking environments. To investigate the molecular basis for the selectivity of the peptides between the bacterial and mammalian cells, we examined the interaction of the peptides with model liposome systems mimicking the bacterial and mammalian cytoplasmic membranes. Furthermore, the molecular mechanism of bacterial-killing action of the peptides was examined by dye leakage from bacterial membrane-mimicking lipid vesicles and membrane depolarization for *Staphylococcus aureus*.

Experimental

Materials. Rink amide 4-methyl benzhydrylamine resin (MBHA) and fluoren-9-ylmethoxycarbonyl (Fmoc) amino acids were purchased from Calibochem-Novabiochem (La Jolla, CA). Other reagents used for peptide synthesis including trifluroacetic acid (TFA; sigma), piperidine (Merck), dicyclohexylcarbodiimide (DCC; Fluka), *N*-hydroxybenzotriazole hydrate (HOBT; Aldrich) and dimethylformamide (DMF, peptide synthesis grade; Biolab). Egg yolk phosphatidylcholine (EYPC), egg yolk phosphatidylglycerol (EYPG), egg yolk phosphatidylethanolamine (EYPE), cholesterol, calcein and gramicidin D (GD) were obtained from Sigma Chemicals (St. Louis, MO). $DiSC_3$-5 was obtained from Molecular Probes (Eugene, OR, USA). All other reagents were of analytical grade.

Synthesis of Fmoc-Nleu. Isobutylamine (7.3 g) was dissolved in 50 mL THF under stirring at room temperature. To the amine solution in an ice-water bath was added ethyl bromoacetate (8.35 g in 20 mL THF) slowly. After 3 h of stirring at room temperature, the reaction mixture was concentrated and the resulting product mixture was purified by column chromatography. The purified substitution product (9.0 g, 57 mmol) was saponified using 4 N-NaOH solution in 100 mL MeOH. After 1 h of stirring at room temperature, the majority of the MeOH was evaporated and the pH was adjusted to 9 using 2 N-HCl solution. Then, Fmoc-OSu (19 g, 57 mmol) in 1,4-dioxane was slowly added with stirring at pH 9. After 1 h of stirring at room temperature, the mixture was treated with extractive work up and was acidified using 2 N-HCl to pH 3. Ethyl acetate was used for extracting the resulting Fmoc-Nleu. The solvent was evaporated and the crude material was purified by column chromatography to give Fmoc-Nleu in 38% overall yield.

Peptide Synthesis. $L_8K_9W_1$ and its analogs were synthesized by the solid phase peptide synthesis using 9-fluorenylmethoxycarbonyl (Fmoc) chemistry. DCC (dicyclohexylcarbodiimide) and HOBt (*N*-hydroxybenzotriazole) were used as coupling reagents, and a 10-fold excess of Fmoc-amino acids was added during every coupling cycle. After cleavage and deprotection with a mixture of trifluoroacetic acid/water/thioanisole/phenol/ethanedithiol/triisopropylsilane

Table 1. Amino acid sequences, calculated and observed molecular masses of $L_8K_9W_1$ and its analogs

Peptides	Amino acid sequences	Molecular mass (Da)	
		Calculated	Observed
$L_8K_9W_1$	KWKKLLKKLLKLLKKLLK-NH_2	2262.1	2262.3
$L_8K_9W_1$-L-Pro	KWKKLLKK**P**LKL**P**KKLLK-NH_2	2230.2	2229.5
$L_8K_9W_1$-D-Pro	KWKKLLKK**P**LKL**P**KKLLK-NH_2	2230.2	2231.2
$L_8K_9W_1$-D-Leu	KWKKLLKK**L**LKL**L**KKLLK-NH_2	2262.1	2262.3
$L_8K_9W_1$-Nleu	KWKKLLKK***l***LKL***l***KKLLK-NH_2	2262.1	2261.9

P: L-Pro, **P**: D-Pro, **L**: D-Leu, ***l***: Nleu [$(CH_3)_2$-CH-NH-CH_2-COOH)] (Peptoid residue for Leu)

(81.5:5:5:5:2.5:1, v/v/v/v/v/v) for 2 h at room temperature, the crude peptide was repeatedly extracted with diethyl ether and purified by RP-HPLC (reverse-phase high-performance liquid chromatography) on a preparative Vydac C_{18} column (20 mm × 250 mm, 300 Å, 15-mm particle size) using an appropriate 0–90% water/acetonitrile gradient in the presence of 0.05% trifluoroacetic acid. The final purity of the peptides (> 95%) was assessed by RP-HPLC on an analytical Vydac C_{18} column (4.6 × 250 mm, 300 Å, 5-mm particle size). Peptides had the correct atomic mass, as determined by matrix-assisted laser desorption/ionization time-of-flight mass spectrometry (MALDI-TOF MS) (Table 1).

Antimicrobial Assay. The antimicrobial activity of the peptides against three Gram-positive bacterial strains, three Gram-negative bacterial strains and three MRSA strains was examined by using the broth microdilution method in sterile 96-well plates. Aliquots (100 μL) of a bacterial suspension at 2×10^6 colony-forming units (CFU)/mL in 1% peptone were added to 100 μL of the peptide solution (serial 2-fold dilutions in 1% peptone). After incubation for 18-20 h at 37 °C, bacterial growth inhibition was determined by measuring the absorbance at 600 nm with a Microplate Autoreader EL 800 (Bio-Tek Instruments, VT). The minimal inhibitory concentration (MIC) was defined as the minimum peptide concentration that inhibited bacteria growth. Three types of Gram-positive bacteria (*Bacillus subtilis* [KCTC 3068], *Staphylococcus epidermidis* [KCTC 1917] and *Staphylococcus aureus* [KCTC 1621]) and three types of Gram-negative bacteria (*Escherichia coli* [KCTC 1682], *Pseudomonas aeruginosa* [KCTC 1637] and *Salmonella typhimurium* [KCTC 1926]) were procured from the Korean Collection for Type Cultures (KCTC) at the Korea Research Institute of Bioscience and Biotechnology (KRIBB). Methicillin-resistant *Staphylococcus aureus* (MRSA) (CCARM 3001 and CCARM 3543) and multidrug-resistant *Pseudomonas aeruginosa* (MDRPA) (CCARM 2095) were obtained from the Culture Collection of Antibiotic-Resistant Microbes (CCARM) at Seoul Women's University in Korea.

Quantification of Hemolytic Activity. Fresh human red blood cells (hRBCs) were centrifuged, washed three times with phosphate-buffered saline (PBS) (35 mM phosphate buffer, 0.15 M NaCl, pH 7.4), dispensed into 96-well plates as100 μL of 4% (w/v) hRBC in PBS, and 100 μL of peptide solution was added to each well. Plates were incubated for 1 h at 37 °C, then centrifuged at 1000 × g for 5 min. Samples (100 μL) of supernatant were transferred to 96-well plates and hemoglobin release was monitored by measuring absorbance at 414 nm. Zero hemolysis was determined in PBS (A_{PBS}) and 100% hemolysis was determined in 0.1% (v/v) Triton X-100 (A_{triton}). The hemolysis percentage was calculated as: % hemolysis = $100 \times [(A_{sample} - A_{PBS})/(A_{triton} - A_{PBS})]$.

Circular Dichroism (CD) Spectroscopy. The CD spectrum of the peptide was obtained with a Jasco J-715 CD spectrophotometer (Tokyo, Japan) at 25 °C using a fused quartz cell with a 1-mm path length over a wavelength range of 190–250 nm at 0.1 nm intervals (speed, 50 nm/min; response time, 0.5 s; bandwidth, 1 nm). CD spectra were collected and averaged over four scans. Samples were prepared by dissolving the peptide to a final concentration of 100 μg/mL in 10 mM sodium phosphate buffer (pH 7.2), 50% (v/v) trifluoroethanol (TFE) or 30 mM sodium dodecyl sulfate (SDS). The mean residue ellipticity [θ] (measured as units of deg × cm^2 × $dmol^{-1}$) was calculated using the formula: $[\theta] = [\theta]_{obs}$ (MRW/10*lc*), where $[\theta]_{obs}$ is the ellipticity measured in millidegrees, MRW is the mean residue molecular weight of the peptide, *c* is the concentration of the sample in mg/mL, and *l* is the optical path length of the cell in cm. Spectra were expressed as molar ellipticity [θ] *versus* wavelength.

Tryptophan Fluorescence and Quenching. Small unilamellar vesicles (SUVs) were prepared for tryptophan fluorescence experiments as described previously.[21] Following chloroform evaporation, the EYPE/EYPG (7:3, w/w) or EYPC/cholesterol (10:1, w/w) lipids were resuspended in 10 mM Tris–HCl buffer (10 mM Tris, pH 7.4, 150 mM NaCl, 0.1 mM EDTA) by vortexing. The lipid dispersions were sonicated in ice water for 20 min using an ultrasonic cleaner until the solutions clarified. Tryptophan fluorescence spectra were measured using an RF 5301 fluorescence spectrophotometer (Shimadzu, Japan). The procedure was performed for each peptide in 10 mM Tris–HCl buffer (pH 7.4) with 500 μM EYPE/EYPG or EYPC/cholesterol lipids. The peptide/lipid molar ratio was 1:50, and the peptide/liposome mixture was allowed to interact for 2 min at 25 °C. An excitation wavelength of 280 nm was used, and emission was scanned at wavelengths ranging from 300 to 400 nm. The spectra were baseline corrected by subtracting blank spectra of the corresponding solutions without the peptide. The quenching of fluorescence was accomplished using acrylamide. To reduce the absorbance of acrylamide, Trp was excited at 295 nm instead of 280 nm. The final concentration of acrylamide was brought to 0.21 M by titrating the 4 M stock solution with liposomes at a lipid/peptide molar ratio of 50:1. The effects of the quenching reagent on peptide fluorescence intensities were assessed by the quenching constant (KSV), which was estimated using the Stern–Volmer equation: $F_0/F = K_{sv}[Q]$, where F_0 and F are the fluorescence values of the peptide in the absence or the presence of acrylamide, respectively, K_{SV} represents the Stern–Volmer quenching constant, and Q represents the concentration of acrylamide.

Dye Leakage. Calcein-entrapped large unilammelar vesicles (LUVs) composed of EYPE/EYPG (7:3, w/w) were prepared by vortexing the dried lipid in a dye buffer solution (70 mM calcein, 10 mM Tris, 150 mM NaCl, 0.1 mM EDTA, pH 7.4). The suspension was subjected to 10 freeze-thaw cycles in liquid nitrogen and extruded 21 times through polycarbonate filters (2 stacked 100-nm pore size filters) with a LiposoFast extruder (Avestin, Inc. Canada). Untrapped calcein was removed by gel filtration on a Sephadex G-50 column. Calcein leakage from LUVs was monitored by measuring the fluorescence intensity at an excitation wavelength of 490 nm and emission wavelength at 520 nm on a model RF-5301PC spectrophotometer. Complete dye release

was obtained using 0.1% Triton X-100.

Membrane Depolarization. The cytoplasmic membrane depolarization activity of the peptides was measured using the membrane potential sensitive dye, $diSC_3$-5 as previously described.[22,23] Briefly, *Staphylococcus aureus* (KCTC 1621) grown at 37 °C with agitation to the mid-log phase (OD_{600} = 0.4) was harvested by centrifugation. Cells were washed twice with washing buffer (20 mM glucose, 5 mM HEPES, pH 7.4) and resuspended to an OD_{600} of 0.05 in similar buffer. The cell suspension was incubated with 20 nM $diSC_3$-5 until stable reduction of fluorescence was achieved, implying incorporation of the dye into the bacterial membrane. Then KCl was added to a final concentration of 0.1 M to equilibrate K^+ levels. Membrane depolarization was monitored by recording changes in the intensity of fluorescence emission of the membrane potential-sensitive dye, $diSC_3$-5 (excitation $\lambda = 622$ nm, emission $\lambda = 670$ nm) after peptide addition. The membrane potential was fully dissipated by adding gramicidin D (final concentration of 0.2 nM). The membrane potential dissipating activity of the peptides is calculated as follows:

$$\% \text{ Membrane depolarization} = 100 \times [(F_p - F_0) / (F_g - F_0)]$$

where F_0 denotes the stable fluorescence value after the addition of the $diSC_3$-5 dye, F_p denotes the fluorescence value 5 min after peptide addition, and F_g denotes the fluorescence signal after gramicidin D (GD) addition.

Results and Discussion

Peptide Synthesis. The structure and molecular weight of the peptides were verified by MALDI-TOF MS. Table 1 summarizes the theoretically calculated and measured molecular weight of each peptide. All peptides had molecular weight values in agreement with their theoretical values, suggesting that the peptides were successfully synthesized.

Antimicrobial Activity. The antimicrobial activities of the peptides were tested in terms of their bacteriostatic inhibitory concentrations, indicated by the MIC, as summarized in Table 2. All $L_8K_9W_1$ analogs displayed the same or 2-8-fold higher antimicrobial activity against all bacterial strains tested compared to $L_8K_9W_1$. The potency of antimicrobial activity of the peptides was ranked according to the geometric mean (GM) of the MICs as follows: $L_8K_9W_1$-Nleu = $L_8K_9W_1$-D-Pro > $L_8K_9W_1$-L-Pro > $L_8K_9W_1$-D-Leu > $L_8K_9W_1$.

Hemolytic Activity. The cytotoxicity of the peptides is often analyzed in terms of their ability to lyse mammalian red blood cells, referred to as hemolysis. The ability of the peptides tested in this study to induce hemolysis of human erythrocytes is summarized in Table 2. Both $L_8K_9W_1$ and $L_8K_9W_1$-D-Leu were found to be relatively highly hemolytic activity ($L_8K_9W_1$ and $L_8K_9W_1$-D-Leu induced 10% hemolysis at 1.36 μM and 1.38 μM, respectively). However, $L_8K_9W_1$-L-Pro, $L_8K_9W_1$-D-Pro and $L_8K_9W_1$-Nleu had no hemolytic activity at concentrations as high as 100 μM.

Antimicrobial Activity Against Antibiotic-resistant Bacteria. We tested the antimicrobial activity of the peptides against methicillin-resistant *Staphylococcus aureus* (MRSA) and multidrug-resistant *Pseudomonas aeruginosa* (MDRPA). As shown in Table 3, $L_8K_9W_1$-L-Pro, $L_8K_9W_1$-D-Pro and $L_8K_9W_1$-Nleu (MIC range, 1 to 4 μM) were more active to MRSA and MDRPA than $L_8K_9W_1$ and $L_8K_9W_1$-D-Leu (MIC range, 4 to 8 μM).

Cell Selectivity. Therapeutic index (TI) is a widely employed parameter to represent the cell selectivity of antimicrobial reagents.[24-26] It was calculated by the ratio of MHC (the peptide concentration that causes 10% hemolysis) and GM (geometric mean of MICs against six bacterial

Table 3. Antimicrobial activities of the peptides against antibiotic-resistant bacteria[a]

Peptides	Minimal Inhibitory Concentration (MIC) (μM)		
	MRSA (CCARM 3001)	MRSA (CCARM 3543)	MDRPA (CCARM 2095)
$L_8K_9W_1$	4	4	4
$L_8K_9W_1$-L-Pro	4	1	2
$L_8K_9W_1$-D-Pro	2	1	2
$L_8K_9W_1$-D-Leu	4	4	8
$L_8K_9W_1$-Nleu	2	1	2

[a]Antibiotic-resistant bacterial strains were clinically isolated at the Culture Collection of Antibiotic-Resistant Microbes (CCARM). MRSA: Methicillin-resistant *Staphylococcus aureus.* MDRPA: multidrug-resistant *Pseudomonas aeruginosa*

Table 2. Minimum inhibitory concentrations (MIC), minimum hemolytic concentrations (MHC), and therapeutic indices (TI) of the peptides

Peptide	Minimal Inhibitory Concentration (MIC)[a] (μM)						GM[b] (μM)	MHC[c] (μM)	TI[d] (MHC/GM)
	Gram-negative bacteria			Gram-positive bacteria					
	E. coli	*P. aeruginosa*	*S. typhimurium*	*B. subtilis*	*S. epidermidis*	*S. aureus*			
$L_8K_9W_1$	4	4	4	4	4	4	4	1.36	0.34
$L_8K_9W_1$-L-Pro	2	1	1	1	1	2	1.33	100 <	150.4
$L_8K_9W_1$-D-Pro	2	1	1	1	0.5	2	1.25	100 <	160.0
$L_8K_9W_1$-D-Leu	4	2	2	2	2	2	2.33	1.38	0.59
$L_8K_9W_1$-Nleu	2	1	1	1	0.5	2	1.25	100 <	160.0

[a]MICs were determined as the lowest concentration of peptide that causes 100% inhibition of microbial growth. [b]The geometric mean (GM) of the peptide MICs against all six bacterial strains was calculated. [c]MHC is the minimum hemolytic concentration that caused 10% hemolysis of human red blood cells (hRBC). When no detectable hemolytic activity was observed at 100 μM, a value of 200 μM was used to calculate the therapeutic index. [d]Therapeutic index (TI) is the ratio of the MHC to the geometric mean of MIC (GM). Larger values indicate greater cell selectivity.

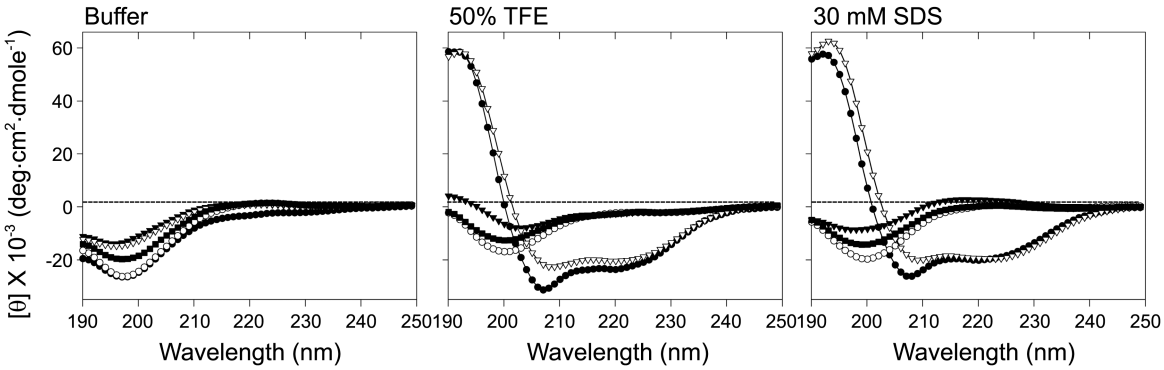

Figure 2. Circular dichroism (CD) spectra of the peptides in 10 mM sodium phosphate buffer (pH 7.4), 50% trifluoroethanol (TFE) or 30 mM sodium dodecyl sulfate (SDS) micelles. Symbols: $L_8K_9W_1$ (●), $L_8K_9W_1$-L-Pro (○), $L_8K_9W_1$-D-Pro (▼), $L_8K_9W_1$-D-Leu (▽) and $L_8K_9W_1$-Nleu (■).

strains). When there was significant no hemolysis at the highest concentration tested (100 μM), 200 μM was used for the TI calculation, since the test was carried out by twofold serial dilution. Larger values in TI indicate greater cell selectivity. As shown in Table 2, $L_8K_9W_1$ and $L_8K_9W_1$-D-Leu had much lower TI of 0.34 and 0.38, respectively, providing poor cell selectivity. In contrast, $L_8K_9W_1$-L-Pro, $L_8K_9W_1$-D-Pro and $L_8K_9W_1$-Nleu exhibited a great TI of 150.4 and 160.0, offering great cell selectivity.

Secondary Structure. Circular dichroism (CD) was performed for all four peptides in different media, including aqueous solutions and membrane-like environments (50% TFE and 30 mM SDS) (Figure 2). In sodium phosphate buffer, all peptides displayed spectra typical of an unordered conformation. In the presence of 50% TFE and 30 mM SDS, $L_8K_9W_1$ and $L_8K_9W_1$-D-Leu displayed the typical α-helical structure characterized by the positive bands near 195 nm and the dichroic minimal values at 205–208 and 222–223

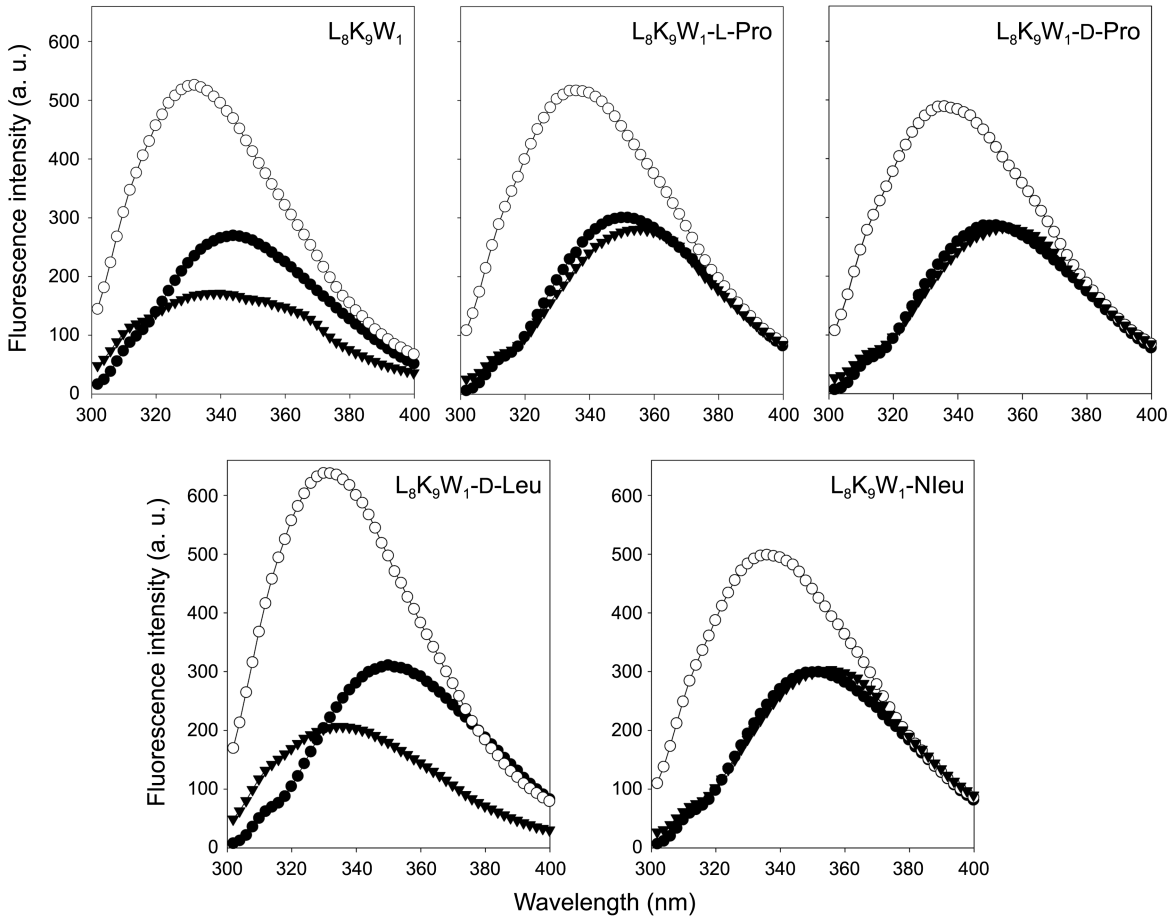

Figure 3. Tryptophan fluorescence emission spectra of the peptides in Tris-buffer (pH 7.4) (●), or in the presence of EYPE/EYPG (7:3, w/w) SUVs (○) and EYPC/cholesterol (10: 1, w/w) SUVs (▼).

Table 4. Fluorescence spectroscopy parameters measured for the peptides in the presence and absence of EYPE/EYPG (7:3, w/w) and EYPC/cholesterol (10:1, w/w) vesicles

Peptide	Fluorescence emission maxima (nm)[a]			K_{SV} [b] (M^{-1})		
	Buffer	EYPE/EYPG	EYPC/cholesterol	Buffer	EYPE/EYPG	EYPC/cholesterol
$L_8K_9W_1$	344	331 (13)	337 (11)	6.34	1.67	0.95
$L_8K_9W_1$-L-Pro	350	335 (15)	350 (0)	6.30	1.99	4.14
$L_8K_9W_1$-D-Pro	350	336 (14)	350 (0)	6.00	1.99	3.69
$L_8K_9W_1$-D-Leu	350	331 (19)	338 (12)	6.54	1.77	0.38
$L_8K_9W_1$-Nleu	350	334 (16)	350 (0)	6.30	1.77	3.76

[a]Blue shift of emission maximum as compared to Tris-buffer. [b]Stern–Volmer constant K_{SV} was calculated by the Stern–Volmer equation: $F_0/F = 1/K_{SV}$ (Q), where Q is the concentration of the quencher (acrylamide). Concentrations of the quencher were increased from 0.03 to 0.21 M. A smaller K_{SV} value reflects a more protected Trp residue.

nm. In contrast, $L_8K_9W_1$-L-Pro, $L_8K_9W_1$-D-Pro and $L_8K_9W_1$-Nleu had an unordered conformation. This result indicated that the double replacement of L-Pro, D-Pro, or Nleu in the hydrophobic face of amphipathic α-helical $L_8K_9W_1$ let to a complete destruction of α-helical structure.

Tryptophan Fluorescence and Quenching. The fluorescence emission characteristics of the Trp residues in the peptides are sensitive to their environment and were used to monitor the binding of peptides to lipid vesicles. The liposomal EYPE/EYPG (7:3, w/w) and EYPC/cholesterol (10:1, w/w) vesicles generally mimic bacterial and eukaryotic membranes, respectively. Fluorescence emission spectra for the tryptophan of the peptides in the presence of phospholipid vesicles are shown in Figure 3. All peptides caused maximal fluorescence emission at approximately 350 nm in aqueous solutions (Table 4). $L_8K_9W_1$ and $L_8K_9W_1$-D-Leu induced larger blue shifts in both EYPE/EYPG (7:3, w/w) and EYPC/cholesterol (10:1, w/w) vesicles, which was consistent with its high antimicrobial activity and high hemolytic activity (Table 4). In contrast, $L_8K_9W_1$-L-Pro, $L_8K_9W_1$-D-Pro and $L_8K_9W_1$-Nleu induced larger blue shifts in EYPE/EYPG (7:3, w/w) but no blue shift in EYPC/cholesterol (10:1, w/w) vesicles, correlating with their high antimicrobial activity and no hemolytic activity (Table 4). The location of the peptides with respect to the bilayer plane was further investigated using fluorescence quenching techniques to create Stern–Volmer plots of the decrease in fluorescence as a function of an added soluble quencher (Figure 4 and Table 4). $L_8K_9W_1$-L-Pro, $L_8K_9W_1$-D-Pro and $L_8K_9W_1$-Nleu had the same low K_{SV} (1.77 and 1.99) in negatively charged vesicles, but much higher K_{SV} (3.76-4.14) in zwitterionic vesicles as compared to $L_8K_9W_1$ and $L_8K_9W_1$-D-Leu, which was in agreement with their greatest cell selectivity (Table 4).

Fluorescent Dye Leakage from Bacterial Membrane Mimicking Liposome. To determine whether the antimicrobial activities of the peptides depend on their capacity to permeate bacterial membranes, we measured their abilities to induce the fluorescent dye calcein leakage from negatively charged EYPE/EYPG (7:3, w/w) large unilamellar vesicles (LUVs), which mimics bacterial membranes. As shown in Figure 5, $L_8K_9W_1$ and $L_8K_9W_1$-D-Leu induced a significant dye leakage (more than 50%) at 1.0 μM. In contrast, $L_8K_9W_1$-L-Pro, $L_8K_9W_1$-D-Pro and $L_8K_9W_1$-Nleu had very little leakage (less than 12%) at concentrations as high as 12.0 μM. This result suggested that bacterial-killing mechanism of $L_8K_9W_1$-L-Pro, $L_8K_9W_1$-D-Pro and $L_8K_9W_1$-Nleu is not due to the disruption/perturbation of bacterial cytoplasmic membranes.

Membrane Depolarization. The membrane potential sensitive dye $diSC_3$-5 was used to monitor the cytoplasmic membrane depolarization of *Staphylococcus aureus* cells in the presence of peptides. This dye is distributed between the cells and medium, depending on the cytoplasmic membrane

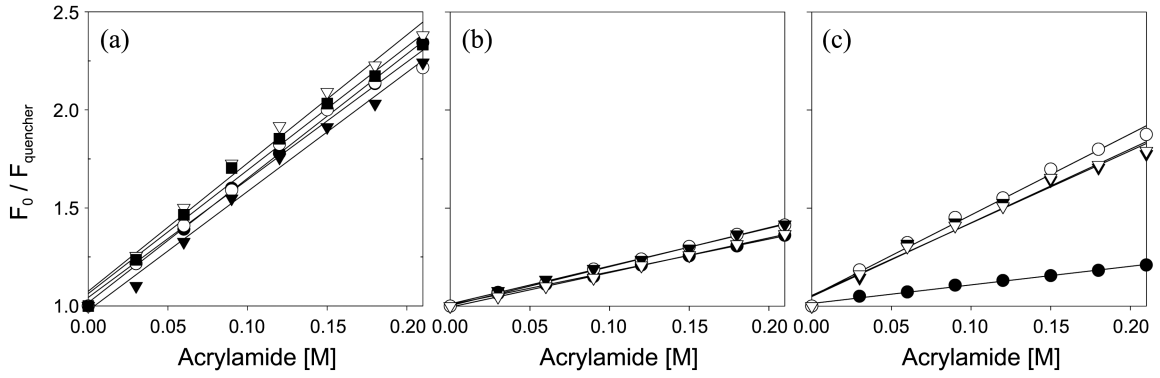

Figure 4. Stern–Volmer plots for the quenching of Trp fluorescence of the peptides by an aqueous quencher, acrylamide, in Tris-buffer (pH 7.4) (a) or in the presence of EYPE/EYPG (7:3, w/w) SUVs (b) and EYPC/cholesterol (10:1, w/w) SUVs (c). Symbols: $L_8K_9W_1$ (●), $L_8K_9W_1$-L-Pro (○), $L_8K_9W_1$-D-Pro (▼), $L_8K_9W_1$-D-Leu (▽) and $L_8K_9W_1$-Nleu (■).

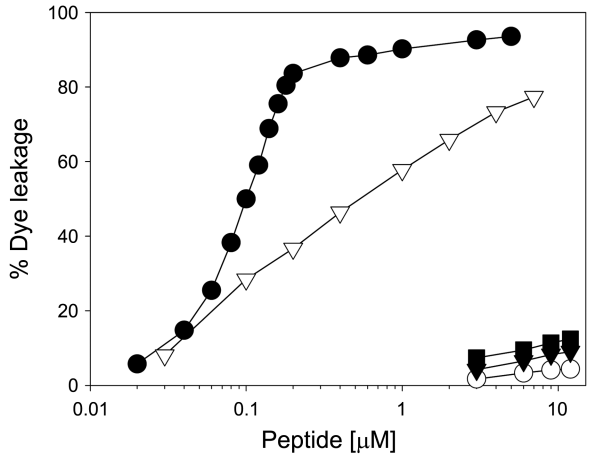

Figure 5. Peptide-induced calcein release from calcein-entrapped negatively charged EYPE/EYPG (7:3, w/w) LUVs. Symbols: $L_8K_9W_1$ (●), $L_8K_9W_1$-L-Pro (○), $L_8K_9W_1$-D-Pro (▼), $L_8K_9W_1$-D-Leu (▽) and $L_8K_9W_1$-Nleu (■).

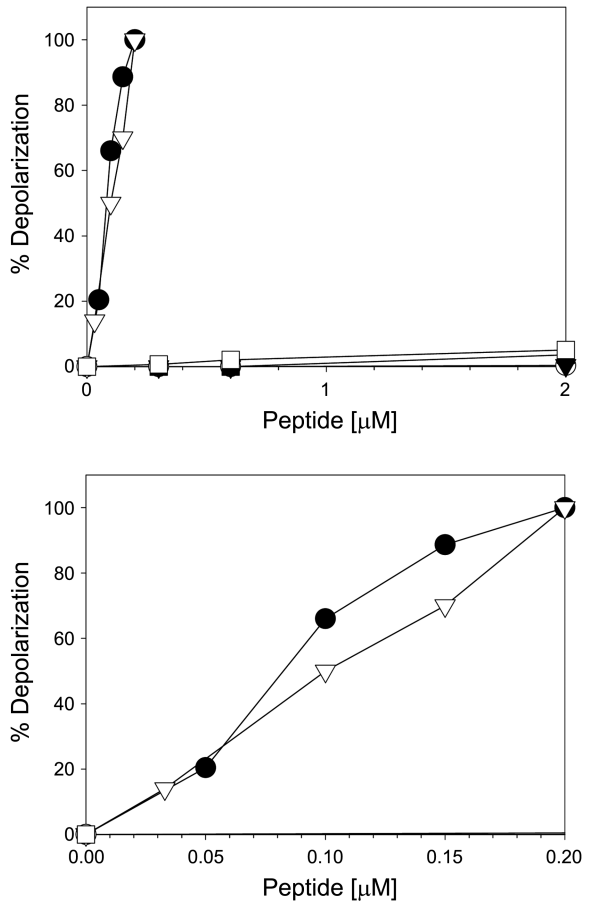

Figure 6. Concentration-dependent, peptide-induced cytoplasmic membrane depolarization against *Staphylococcus aureus*. Membrane depolarization was measured by an increase in fluorescence of the potentiometric fluorescent dye $diSC_3$-5. Dye release was monitored at an excitation wavelength of 622 nm and an emission wavelength of 670 nm. Symbols: $L_8K_9W_1$ (●), $L_8K_9W_1$-L-Pro (○), $L_8K_9W_1$-D-Pro (▼), $L_8K_9W_1$-D-Leu (▽) and $L_8K_9W_1$-Nleu (■).

potential, and self-quenches when concentrated inside bacterial cells. If the membrane is depolarized, the probe will be

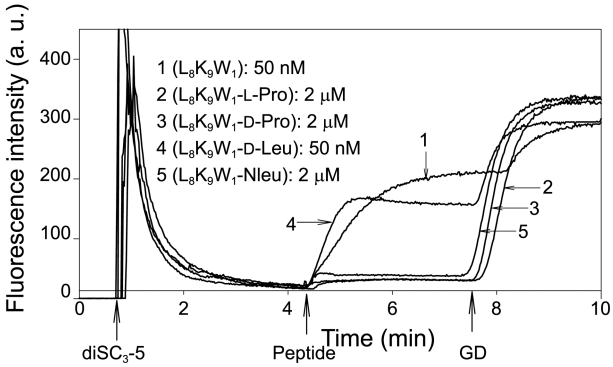

Figure 7. Time-dependent, peptide-induced cytoplasmic membrane depolarization against *Staphylococcus aureus*. Membrane depolarization was measured by an increase in fluorescence of the membrane potential–sensitive dye, $diSC_3$-5. Dye release was monitored at an excitation wavelength of 622 nm and an emission wavelength of 670 nm. In each run, the peptides were added near the 4.4-min mark.

released into the medium, causing a measurable increase in fluorescence. Both $L_8K_9W_1$ and $L_8K_9W_1$-D-Leu induced a complete membrane depolarization at 0.2 μM (Figures 6 and 7). In contrast, $L_8K_9W_1$-L-Pro, $L_8K_9W_1$-D-Pro and $L_8K_9W_1$-Nleu caused no or less membrane depolarization even at 2 μM (Figures 6 and 7). This result suggested that $L_8K_9W_1$-L-Pro, $L_8K_9W_1$-D-Pro and $L_8K_9W_1$-Nleu did not kill microorganisms by the formation of pore/ion channels on bacterial cell membranes

Conclusion

In this study, we have confirmed that the double replacement of L-Pro, D-Pro or Nleu in the hydrophobic face (positions 9 and 13) of non-cell-selective AMP $L_8K_9W_1$ let to a great increase in the selectivity toward bacterial cells and a complete destruction of α-helical structure. Interestingly, $L_8K_9W_1$-L-Pro, $L_8K_9W_1$-D-Pro and $L_8K_9W_1$-Nleu do not disrupt membranes to a large enough extent to allow for leakage of calcein from bacterial membrane-mimicking LUVs or extensive membrane depolarization. These results suggested that the mode of action of $L_8K_9W_1$-L-Pro, $L_8K_9W_1$-D-Pro and $L_8K_9W_1$-Nleu involves the intracellular target other than the bacterial membrane. In particular, $L_8K_9W_1$-L-Pro, $L_8K_9W_1$-D-Pro and $L_8K_9W_1$-Nleu displayed strong antimicrobial activity (MIC range, 1 to 4 μM) against MRSA and MDRPA. Taken together, our results suggested that $L_8K_9W_1$-L-Pro, $L_8K_9W_1$-D-Pro and $L_8K_9W_1$-Nleu with great cell selectivity appear to be promising candidates for future development as novel antimicrobial agents.

Acknowledgments. This study was supported by the research fund from Chosun University, 2013.

References

1. Zasloff, M. *Nature* **2002**, *415*, 389.
2. Hancock, R. E.; Scott, M. G. *Proc. Natl. Acad. Sci. USA* **2000**, *97*,

8856.
3. Hancock, R. E.; Diamond, G. *Trends Microbiol.* **2000**, *8*, 402.
4. Andreu, D.; Merrifield, R. B.; Steiner, H.; Boman, H. G. *Biochemistry* **1985**, *24*, 1683.
5. Maloy, W. L.; Kari, U. P. *Biopolymers* **1995**, *37*, 105.
6. Blondelle, S. E.; Simpkins, L. R.; Perez-Paya, E.; Houghten, R. A. *Biochim. Biophys. Acta* **1993**, *1202*, 331.
7. Thennarasu, S.; Nagaraj, R. *Protein Eng.* **1996**, *9*, 1219.
8. Shai, Y. *Biopolymers* **2002**, *66*, 236.
9. Papo, N.; Shai, Y. *Peptides* **2003**, *24*, 1693.
10. Kang, S. J.; Won, H. S.; Choi, W. S.; Lee, B. J. *J. Pept. Sci.* **2009**, *15*, 583.
11. Fernandez, D. I.; Sani, M. A.; Gehman, J. D.; Hahm, K. S.; Separovic, F. *Eur. Biophys. J.* **2011**, *40*, 471.
12. Wang, P.; Nan, Y. H.; Yang, S. T.; Kang, S. W.; Kim, Y.; Park, I. S.; Hahm, K. S.; Shin, S. Y. *Peptides* **2010**, *31*, 1251.
13. Epand, R. F.; Lehrer, R. I.; Waring, A.; Wang, W.; Maget-Dana, R.; Lelièvre, D.; Epand, R. M. *Biopolymers* **2003**, *71*, 2.
14. Dathe, M.; Meyer, J.; Beyermann, M.; Maul, B.; Hoischen, C.; Bienert, M. *Biochim. Biophys. Acta* **2002**, *1558*, 171.
15. Agawa,Y.; Lee, S.; Ono, S.; Aoyagi, H.; Ohno, M.; Taniguchi, T.; Anzai, K.; Kirino, Y. *J. Biol. Chem.* **1991**, *266*, 20218.
16. Kiyota, T.; Lee, S.; Sugihara, G. *Biochemistry* **1996**, *35*, 13196.
17. Beven, L.; Castano, S.; Dufourcq, J.; Wieslander, A.; Wroblewski, H. *Eur. J. Biochem.* **2003**, *270*, 2207.
18. Yin, L. M.; Edwards, M. A.; Li, J.; Yip, C. M.; Deber, C. M. *J. Biol. Chem.* **2012**, *287*, 7738.
19. Wang, P.; Nan, Y. H.; Shin, S. Y. *J. Pept. Sci.* **2010**, *16*, 601.
20. Song, Y. M.; Yang, S. T.; Lim, S. S.; Kim, Y.; Hahm, K. S.; Kim, J. I.; Shin, S. Y. *Biochem. Biophys. Res. Commun.* **2004**, *314*, 615.
21. Lee, K. H.; Lee, D. G.; Park, Y.; Kang, D. I.; Shin, S. Y.; Hahm, K. S.; Kim, Y. *Biochem. J.* **2006**, *394*, 105.
22. Friedrich, C. L.; Moyles, D.; Beveridge, T. J.; Hancock, R. E. *Antimicrob. Agents Chemother.* **2000**, *44*, 2086.
23. Friedrich, C. L.; Rozek, A.; Patrzykat, A.; Hancock, R. E. *J. Biol. Chem.* **2001**, *276*, 24015.
24. Chen, Y.; Mant, C. T.; Farmer, S. W.; Hancock, R. E.; Vasil, M. L.; Hodges, R. S. *J. Biol. Chem.* **2005**, *280*, 12316.
25. Fázio, M. A.; Jouvensal, L.; Vovelle, F.; Bulet, P.; Miranda, M. T.; Daffre, S.; Miranda, A. *Biopolymers* **2007**, *88*, 386.
26. Nan, Y. H.; Bang, J. K.; Jacob, B.; Park, I. S.; Shin, S. Y. *Peptides* **2012**, *35*, 239.